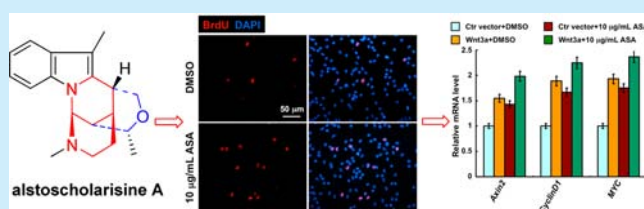


## Indole Alkaloids with New Skeleton Activating Neural Stem Cells

Xing-Wei Yang,<sup>†,§,||</sup> Cui-Ping Yang,<sup>‡,||</sup> Li-Ping Jiang,<sup>‡,§</sup> Xu-Jie Qin,<sup>†,§</sup> Ya-Ping Liu,<sup>†</sup> Qiu-Shuo Shen,<sup>‡,§</sup> Yong-Bin Chen,<sup>\*,‡</sup> and Xiao-Dong Luo<sup>\*,†</sup><sup>†</sup>State Key Laboratory of Phytochemistry and Plant Resources in West China, Kunming Institute of Botany, Chinese Academy of Sciences, Kunming 650201, People's Republic of China<sup>‡</sup>Key Laboratory of Animal Models and Human Disease Mechanisms, Kunming Institute of Zoology, Chinese Academy of Sciences, Kunming 650223, People's Republic of China<sup>§</sup>University of Chinese Academy of Sciences, Beijing 100049, People's Republic of China

## Supporting Information

**ABSTRACT:** Alstoscholarisines A–E (1–5), five unprecedented monoterpene indole alkaloids with 6/5/6/6/6 fused-bridge rings, were isolated from *Alstonia scholaris*. They promoted adult neuronal stem cells (NSCs) proliferation significantly, in which the most active one (1) functioned from a concentration of 0.1  $\mu\text{g}/\text{mL}$  in a dosage-dependent manner. Furthermore, 1 enhanced NSC sphere formation and neurogenic fate commitment through activation of a Wnt signaling pathway and promoted NSC differentiation but did not affect proliferation of neuroblastoma cells.



It has been now well accepted that all mammalian species, including humans, consistently sustain reservoirs of neuronal stem/progenitor cells (NSCs) in the subventricular zone and the subgranular zone of the hippocampal dentate gyrus.<sup>1</sup> The maintenance and differentiation of NSCs in these two areas are important for the formation of new neurons.<sup>2</sup> Many neurogenic disorders, such as Alzheimer's and Parkinson's diseases, are characterized by a progressive loss of neuronal activity.<sup>3</sup> Novel approaches aimed at restoration of neuronal viability or at prevention of neuronal decline are in high demand. In addition, many of the genetic and biochemical pathways which regulate adult hippocampal neurogenesis have been investigated.<sup>4</sup> However, identifying small molecules that modulate hippocampal NSCs activity is still under explored, which might be valuable to gain proof of concept that stem cell expansion strategy will be therapeutically useful.

In recent years, a few small molecules which modulated NSC proliferation or cell fate choice have been identified.<sup>5</sup> Natural products endowed with pivotal neuromodulatory activity and chemical structure scaffold inspiring the design and synthesis of compounds with better biological activity have attracted more attention.<sup>3,6</sup> Total alkaloids from the leaves of *Alstonia scholaris* promoted NSC proliferation during our preliminary screening. Then the phytochemical investigation of the total alkaloids led to the isolation of alstoscholarisines A–E (1–5, Figure 1), five novel monoterpene indole alkaloids (MIAs) possessing 6/5/6/6/6 complicated rings with five continuous chiral centers. Their structures were determined by extensive spectroscopic data and single-crystal X-ray diffractions. All of the compounds promoted adult NSC proliferation significantly, in which the most active one (1) functioned from a concentration of 0.1  $\mu\text{g}/\text{mL}$  in a dosage-dependent manner. Furthermore, 1 enhanced

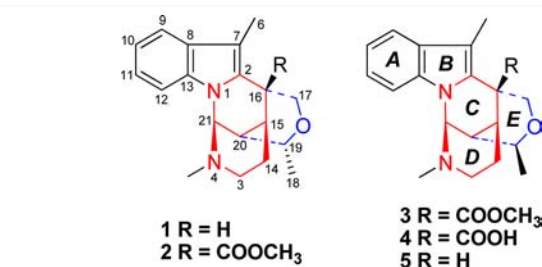


Figure 1. Structures of compounds 1–5.

NSC sphere formation and neurogenic fate commitment at least partially through activating a Wnt signaling pathway.

Alstoscholarisine A (1) afforded as a colorless crystal that exhibited a molecular ion peak at  $m/z$  296.1890 in its HREIMS spectrum, which in conjunction with the <sup>13</sup>C NMR spectral data (Table S1, Supporting Information) indicated a molecular formula of C<sub>19</sub>H<sub>24</sub>N<sub>2</sub>O. The UV spectrum showed maximal absorptions of an indole chromophore (233 and 287 nm).<sup>7</sup> The <sup>13</sup>C NMR and DEPT spectra revealed 19 carbon signals due to five methines ( $\delta_{\text{C}}$  34.5, 35.8, 43.0, 67.7, and 75.3), three methylenes ( $\delta_{\text{C}}$  31.1, 47.3, and 74.3), three methyls ( $\delta_{\text{C}}$  8.1, 18.7, and 45.6), and other eight signals typically assignable to a substituent indole ring moiety. The spectral data together with a series of MIAs from *A. scholaris* suggested that 1 might be a MIA derivative.<sup>7,8</sup> Unlike other intact MIAs, the correlation of  $\delta_{\text{H}}$  2.21 (3H, s, Me-6) with  $\delta_{\text{C}}$  136.9 (C-2), 105.0 (C-7), and 130.2 (C-8) in the HMBC spectrum of 1 suggested an

Received: October 3, 2014

Published: October 29, 2014

uncommon methyl (Me-6) attached to C-7 of the indole ring directly (Figure 2).

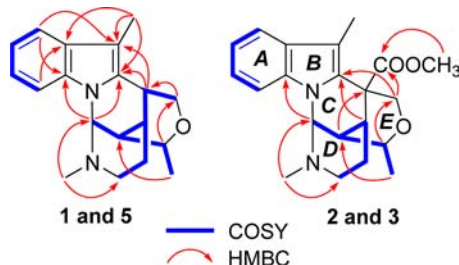


Figure 2. HMBC and  $^1\text{H}$ - $^1\text{H}$  COSY correlations of 1–3 and 5.

In the HMBC spectrum, the correlations of a downfield proton  $\delta_{\text{H}}$  5.47 (d,  $J = 2.6$  Hz, H-21) with  $\delta_{\text{C}}$  136.9 (C-2) and 138.5 (C-13) indicated the direct connection between C-21 and N-1. Furthermore, the correlation of  $\delta_{\text{H}}$  5.47 (H-21)/2.12 (H-20)/2.18 (H-15)/3.03 (H-16) in the  $^1\text{H}$ - $^1\text{H}$  COSY spectrum, as well as the correlations from  $\delta_{\text{H}}$  3.03 (H-16) to  $\delta_{\text{C}}$  136.9 (C-2) and 105.0 (C-7) in the HMBC spectrum, established a six-membered ring-C. The cross peaks of a singlet methyl at  $\delta_{\text{H}}$  2.24 (attributable to N4-Me with corresponding chemical shift at  $\delta_{\text{C}}$  45.6 in the  $^{13}\text{C}$  NMR spectrum) with  $\delta_{\text{C}}$  67.7 (C-21) and a methylene at  $\delta_{\text{C}}$  47.3 (C-3) in the HMBC spectrum suggested the linkage of C-21/N-4/C-3 (Figure 2). The deduction could explain the downfield chemical shifts of H-21 ( $\delta_{\text{H}}$  5.47) and C-21 ( $\delta_{\text{C}}$  67.7) in the  $^1\text{H}$  and  $^{13}\text{C}$  NMR spectrum, respectively, for C-21 connecting two nitrogen atoms. Correlations of  $\delta_{\text{H}}$  2.03, 1.74 (2H, H-14)/2.18 (H-15), and of  $\delta_{\text{H}}$  2.03, 1.74 (H-14)/1.84, 2.30 (2H, H-3) in the  $^1\text{H}$ - $^1\text{H}$  COSY spectrum, together with the established linkage of C-21/20/15, constructed the six-membered ring-D. The linkages of C-18/19/20 and C-16/17 were indicated by the correlations of  $\delta_{\text{H}}$  1.22 (Me-18) with  $\delta_{\text{H}}$  3.69 (H-19), of  $\delta_{\text{H}}$  3.69 with  $\delta_{\text{H}}$  2.12 (H-20), and of  $\delta_{\text{H}}$  3.03 (H-16) with  $\delta_{\text{H}}$  3.57 (H-17) in the  $^1\text{H}$ - $^1\text{H}$  COSY spectrum. Then, a six-membered ether ring-E was proposed by the downfield chemical shift of C-17 ( $\delta_{\text{C}}$  74.3) and C-19 ( $\delta_{\text{C}}$  75.3), combined with the cross peak between  $\delta_{\text{H}}$  3.69 and  $\delta_{\text{C}}$  75.3 in the HMBC spectrum, which met its degrees of unsaturation. Thus, the planar structure of 1 was elucidated to possess an unprecedented 6/5/6/6/6 ring-fused system.

In a molecular model, the rigid structure required the single bonds of C-15/14 and C-21/N-4 located axially in chair ring-C to form the six-membered ring-D. Likewise, to form the six-membered ring-E, the single bonds of C-16/17 and C-20/19 should locate axially in chair ring-C. Then, rings D and E should be placed at different sides of C-ring, respectively, and bridgehead H-15, 16, 20, and 21 were positioned equatorially. Furthermore, the final refinement on the Cu  $K\alpha$  data of crystal of 1 [CCDC 1015370, the Hooft parameter is 0.13(7) for 1105 Bijvoet pairs] unambiguously confirmed the structure of 1,<sup>9</sup> in which rings C, D, and E were all appeared as the chair conformation to avoid steric hindrance. In the fused-bridge ring system, ring D was located at the top side of the plane of the A, B, C-ring system and ring-E at the bottom side. Then, the absolute configuration of 1 was determined as 1*S*,16*R*,19*R*,20*S*,21*S* (Figure 3).

The molecular formula of alstoscholarisine B (2) was established to be  $\text{C}_{21}\text{H}_{26}\text{N}_2\text{O}_3$  by HREIMS ( $m/z$  354.1940,  $\text{M}^+$ ) and the  $^{13}\text{C}$  NMR spectral data (Table S1, Supporting

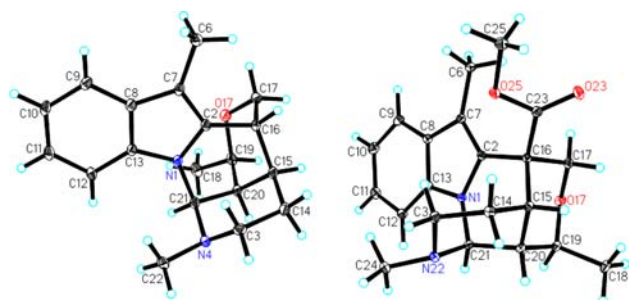


Figure 3. X-ray crystallographic structures of 1 and 3.

Information), which was 68 mass units more than that of 1. Upon comparison of the  $^1\text{H}$  and  $^{13}\text{C}$  NMR spectral data of 1 and 2, an extra carboxymethyl group at  $\delta_{\text{C}}$  173.3 (s), 52.1 (q) and corresponding protons at  $\delta_{\text{H}}$  3.87 (3H, s) appeared in 2. In addition, the absence of a methine ( $\delta_{\text{C}}$  35.8, C-16) and the presence of a quaternary carbon at  $\delta_{\text{C}}$  48.8 (C-16) in the  $^{13}\text{C}$  NMR spectrum of 2 suggested that the carboxymethyl group was attached to C-16. The suggestion was further supported by the correlations of  $\delta_{\text{H}}$  3.75 (H-17) with  $\delta_{\text{C}}$  48.8 (C-16) and 173.3 ( $-\text{COOCH}_3$ ) in its HMBC spectrum. Other parts of 2 were identical to those of 1 by detailed analysis of 2D NMR spectroscopic data of 2.

Alstoscholarisine C (3) shared the same planar scaffold as 2 by detailed analysis of its HREIMS and extensive NMR spectral data (Tables S1 and S2, Supporting Information). Comparison of the  $^{13}\text{C}$  NMR spectra of 2 and 3, about 6 ppm upfield shifts for both C-15 ( $\delta_{\text{C}}$  33.5) and C-17 ( $\delta_{\text{C}}$  68.9), and 5 ppm downfield shift for C-21 ( $\delta_{\text{C}}$  71.8) in 3, suggested that 3 might be 19-epimer of 2. The suggestion was further supported by the NOE correlation of  $\delta_{\text{H}}$  3.94 (H-19) with  $\delta_{\text{H}}$  5.38 (H-21), and of  $\delta_{\text{H}}$  1.28 (Me-18) with  $\delta_{\text{H}}$  2.57 (H-15) in its ROESY spectrum. Finally, the single-crystal X-ray of 3 (CCDC 963511) confirmed its structure with relative configuration.

Alstoscholarisine D (4) was assigned the molecular formula of  $\text{C}_{20}\text{H}_{24}\text{N}_2\text{O}_3$  by HREIMS ( $m/z$  340.1780,  $\text{M}^+$ ), 14 mass units less than 3. Comprehensive analysis of the 1D and 2D NMR spectral data (Tables S1 and S2, Supporting Information) suggested that 4 was a demethyl derivative of 3. Likewise, alstoscholarisine E (5) was elucidated to be a decarboxymethyl derivative of 3 on the basis of the detailed analysis of its HREIMS and extensive NMR spectral data. The relative configurations of 4 and 5 were the same as that of 3 indicated by their ROESY spectra. The similar experimental CD curves of compounds 1–5 (Figure S1, Supporting Information) proposed the absolute configurations of 2–5 based on the X-ray analysis of 1. The plausible biosynthesis pathways of 1–5 were also proposed in Scheme S1 in the Supporting Information.

All of the isolated alkaloids and the total alkaloids (TA) were evaluated for their bioactivities of regulating hippocampal NSC proliferation in vitro (Supporting Information). The results indicated that compounds 1–5 at 10  $\mu\text{g}/\text{mL}$  whereas TA at 30  $\mu\text{g}/\text{mL}$  were able to enhance NSC proliferation significantly using SRB assay in basal medium supplemented with 10 ng/mL basic fibroblast growth factor (bFGF) (Figure 4A). Alstoscholarisine A (ASA), the most potential compound, worked alone or together with bFGF to promote NSCs survival and proliferation in a dosage-dependent manner at the lowest working conditions close to 0.1  $\mu\text{g}/\text{mL}$  (Figure 4B). Then, the unaffected proliferation rates in mouse neuroblastoma cells

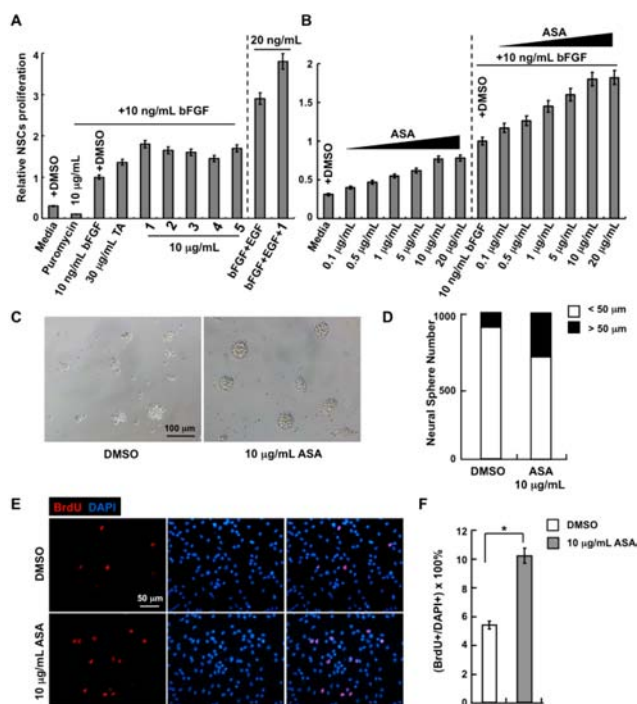


**Figure 4.** Alstoscholarisine (1–5)-promoted hippocampal NSC proliferation. (A and B) Mouse hippocampal NSCs cell proliferation assay by SRB; the relative proliferation is shown compared to the 10 ng/mL bFGF, which is set to 1; ASA: alstoscholarisine A (1). (C and D) Hippocampal NSCs neurosphere cultures; D is the quantification results for C; scale bar: 100  $\mu\text{m}$ . (E and F) BrdU incorporation assay; F is the quantification results for E; scale bar: 50  $\mu\text{m}$ ,  $p \leq 0.05$ ).

(Neuro2a) and fibroblast cells (NIH 3T3) indicated that the activity for **1** might be NSC specific (Figure S5A, Supporting Information). To further evaluate NSCs' self-renew ability affected by **1**, the neurosphere formation assay was performed, and the number of neurospheres over 50  $\mu\text{m}$  in diameter was 3 times more in the presence of **1** than that treated by DMSO (Figure 4C,D). In addition, there was 2 times more BrdU-positive NSCs in the presence of **1** than that in DMSO in the BrdU incorporation assays (Figure 4E,F).

Since the apoptotic signaling pathways induced by TNF $\alpha$  in NSCs was not affected by **1** (Figure S2, Supporting Information), the microarray analysis to gain the genome-wide transcriptional perspective in NSCs were used to uncover the underlying mechanisms for **1** enhancing NSC proliferation (Supporting Information). Upon comparison of the transcriptome profile with DMSO treatment, a total of 3149 genes were dis-regulated (1847 up and 1302 down, Table S3, Supporting Information). Interestingly, some genes involved in Wnt and Hedgehog (Hh) signaling pathways were affected, which are highly conserved to modulate both embryonic nervous system development and adult neurogenesis.<sup>4</sup> Then, the Wnt signaling transduction by TOPFlash luciferase reporter assay revealed that **1** alone or together with Wnt3a were able to activate TOPFlash, whereas **1** has no synergistic effect with LiCl (a GSK3 $\beta$  inhibitor) or  $\Delta\text{N}$ - $\beta$ -catenin (a constitutive active form of  $\beta$ -catenin). The results suggested that **1** acted upstream of the  $\beta$ -catenin degradation complex (Figure 5A). In addition, endogenous Wnt target genes, such as *Axin2*, *CyclinD1*, and *MYC*, were activated by **1** alone or together with Wnt3a (Figure 5B).<sup>10</sup> In contrast, the Hh signaling reporter *8XGli-BS-Luc* did not respond to **1** except for about 2-

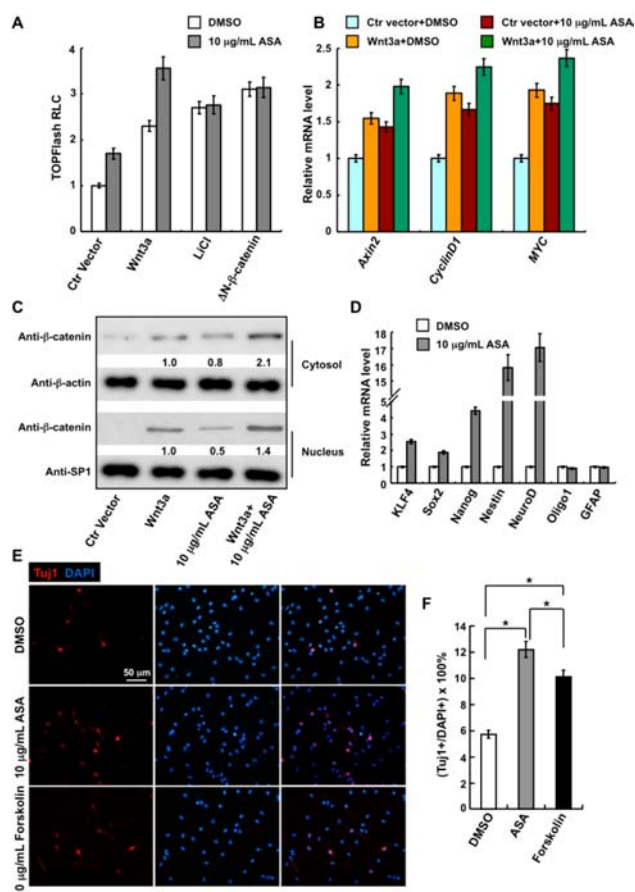


**Figure 5.** Alstoscholarisine A (ASA) activated Wnt signaling and increased NSCs neurogenic fate commitment. (A and B) ASA activated Wnt signaling response luciferase reporter TOPFlash and downstream genes *Axin2*, *CyclinD1*, *MYC* in a Wnt ligand-independent manner and had synergistic effect with Wnt3a; qRT-PCR was normalized to *GAPDH* expression; Ctr = control. (C) ASA synergized with Wnt3a to stabilize cytosolic and nuclear  $\beta$ -catenin. Values are given beneath each band which was normalized to Wnt3a treatment (set to 1). (D) Expression of indicated genes was determined by qRT-PCR and normalized to *GAPDH* expression. (E and F) Hippocampal NSCs differentiation assay was performed and the cells were stained for Tuj1 and DAPI; F is the quantification results for E; scale bar: 100  $\mu\text{m}$ ,  $p \leq 0.05$ ).

fold up-regulation of *Ptch1* and slightly down-regulation of *Gli1* (Figure S3, Supporting Information),<sup>11</sup> which suggested that Hh signaling pathway might not be critical for the NSCs activation by **1**. Consistently, **1** alone or together with Wnt3a increased both cytosolic and nuclear  $\beta$ -catenin protein level (Figure 5C). The results suggested that **1** increased NSCs proliferation at least in part through activating a Wnt signaling pathway.

In our qRT-PCR verification data, *KLF4*, *Sox2*, *Nanog*, and *Nestin* were all unanimously increased, whereas the *Oligo1* and *GFAP* were barely changed (Figure 5D), implying that **1** could be important to maintain the NSCs stemness. It is worthy to note that *NeuroD* was up-regulated dramatically treated by **1**, which suggested that the neuronal fate commitment for NSCs could be affected by **1** as well. The hypothesis was supported by the neuronal differentiation assay.<sup>12</sup> There was two times more of the ratio of Tuj1+/total cells treated by **1** compared with DMSO and 20% more compared with 10  $\mu\text{g}/\text{mL}$  of forskolin, a well-known NSCs neuronal differentiation inducing factor

(Figure SE–F). However, the ratio for GFAP+/total cells was not changed (Figure S4, Supporting Information). These data indicated that **1** promoted NSCs preferential differentiation into neuron, which could be used to integrate with existing neural circuit in order to compensate neurodegenerative damages.<sup>13</sup> Interestingly, the neuroblastoma cell (Neuro2a) proliferation was not affected by **1**, but the neurite outgrowth which is a critical state of neuronal differentiation was boosted more than 2-fold compared with DMSO (Figure SSB,C, Supporting Information).

Alstoscholarisine A might provide great insight into the mechanism involved in the regulation of adult hippocampal NSCs, which could potentially be useful in future studies modulating neurogenesis or neuroblastoma in the adult brain. There is huge scientific and clinical interest in identifying external factors that could be used to promote NSC proliferation and neuronal differentiation, which raises the hope for stem cell based therapies to restore brain functions due to neurodegenerative diseases.<sup>14</sup> Our findings present challenging natural products for organic synthesis and also might provide a clue for the treatment of neurogenic disorders, i.e., Alzheimer's disease, Parkinson's disease, and Huntington's disease.

## ■ ASSOCIATED CONTENT

### ■ Supporting Information

Details of isolation and biological experimental procedures, MS and NMR spectra, crystallographic file (CIF), and microarray data (Excel). This material is available free of charge via the Internet at <http://pubs.acs.org>.

## ■ AUTHOR INFORMATION

### Corresponding Authors

\*E-mail: [xdluo@mail.kib.ac.cn](mailto:xdluo@mail.kib.ac.cn).

\*E-mail: [ybchen@mail.kiz.ac.cn](mailto:ybchen@mail.kiz.ac.cn).

### Author Contributions

<sup>||</sup>These authors contributed equally.

### Notes

The authors declare no competing financial interest.

## ■ ACKNOWLEDGMENTS

We are grateful to the National Natural Science Foundation of China (81225024, 81322030), the Ministry of Science and Technology of China (2014ZX09301307-003), and the Chinese Academy of Sciences (West Light Foundation and XDB13000000) for partial financial support.

## ■ REFERENCES

- (1) Gross, C. G. *Nat. Rev. Neurosci.* **2000**, *1*, 67–73.
- (2) (a) van Praag, H.; Kempermann, G.; Gage, F. H. *Nat. Neurosci.* **1999**, *2*, 266–270. (b) Zhao, C.; Deng, W.; Gage, F. H. *Cell* **2008**, *132*, 645–660.
- (3) Antonchick, A. P.; López-Tosco, S.; Parga, J.; Sievers, S.; Schürmann, M.; Preut, H.; Höing, S.; Schöler, H. R.; Sternecker, J.; Rauh, D.; Waldmann, H. *Chem. Biol.* **2013**, *20*, 500–509.
- (4) Mu, Y.; Lee, S. W.; Gage, F. H. *Curr. Opin. Neurobiol.* **2010**, *20*, 416–423.
- (5) (a) Schneider, J. W.; Gao, Z.; Li, S.; Farooqi, M.; Tang, T. S.; Bezprozvanny, I.; Frantz, D. E.; Hsieh, J. *Nat. Chem. Biol.* **2008**, *4*, 408–410. (b) Pieper, A. A.; Xie, S.; Capota, E.; Estill, S. J.; Zhong, J.; Long, J. M.; Becker, G. L.; Huntington, P.; Goldman, S. E.; Shen, C. H.; Capota, M.; Britt, J. K.; Kotti, T.; Ure, K.; Brat, D. J.; Williams, N.

S.; MacMillan, K. S.; Naidoo, J.; Melito, L.; Hsieh, J.; Brabander, J. D.; Ready, J. M.; McKnight, S. L. *Cell* **2010**, *142*, 39–51. (c) Yang, Y. M.; Gupta, S. K.; Kim, K. J.; Powers, B. E.; Cerqueira, A.; Wainger, B. J.; Ngo, H. D.; Rosowski, K. A.; Schein, P. A.; Ackeifi, C. A.; Arvanites, A. C.; Davidow, L. S.; Woolf, C. J.; Rubin, L. L. *Cell Stem Cell* **2013**, *12*, 713–726.

(6) (a) Carcache, D. A.; Cho, Y. S.; Hua, Z.; Tian, Y.; Li, Y. M.; Danishefsky, S. J. *J. Am. Chem. Soc.* **2006**, *128*, 1016–1022. (b) Jessen, H. J.; Schumacher, A.; Shaw, T.; Pfaltz, A.; Gademann, K. *Angew. Chem., Int. Ed.* **2011**, *50*, 4222–4226.

(7) Feng, T.; Cai, X. H.; Zhao, P. J.; Du, Z. Z.; Li, W. Q.; Luo, X. D. *Planta Med.* **2009**, *75*, 1537–1541.

(8) (a) Cai, X. H.; Du, Z. Z.; Luo, X. D. *Org. Lett.* **2007**, *9*, 1817–1820. (b) Cai, X. H.; Tan, Q. G.; Liu, Y. P.; Feng, T.; Du, Z. Z.; Li, W. Q.; Luo, X. D. *Org. Lett.* **2008**, *10*, 577–580. (c) Cai, X. H.; Liu, Y. P.; Feng, T.; Luo, X. D. *Chin. J. Nat. Med.* **2008**, *6*, 20–22.

(9) Hooft, R. W. W.; Straver, L. H.; Spek, A. L. *J. Appl. Crystallogr.* **2008**, *4*, 96–103.

(10) Mao, Y.; Ge, X.; Frank, C. L.; Madison, J. M.; Koehler, A. N.; Doud, M. K.; Tassa, C.; Berry, E. M.; Soda, T.; Singh, K. K.; Biechele, T.; Petryshen, T. L.; Moon, R. T.; Haggarty, S. J.; Tsai, L. H. *Cell* **2009**, *136*, 1017–1031.

(11) Chen, Y.; Sasai, N.; Ma, G.; Yue, T.; Jia, J.; Briscoe, J.; Jiang, J. *PLoS Biol.* **2011**, *9*, e1001083.

(12) Hsieh, J.; Aimone, J. B.; Kaspar, B. K.; Kuwabara, T.; Nakashima, K.; Gage, F. H. *J. Cell Biol.* **2004**, *164*, 111–122.

(13) Mu, Y.; Gage, F. H. *Mol. Neurodegener.* **2011**, *6*, 85.

(14) Reynolds, B. A.; Rietze, R. L. *Nat. Methods* **2005**, *2*, 333–336.